The influence of ice rubble on sea ice friction
Experimental evidence on the centimetre and metre scales.

Abstract
Sea ice floes in the Arctic collide with each other, and this leads to the production of smaller pieces of broken ice, which we call rubble. Rubble is also produced when ice collides with offshore structures, and when ships pass through sea ice. Previous analyses of ice friction have considered the contact between two sliding ice surfaces. Here, we consider the effective friction between two ice surfaces separated by ice rubble. In particular, we present experimental results across a range of scales and environments. We show results from metre-scale experiments in the Barents Sea; from metre-scale experiments in the Hamburg Ship Model Basin (HSVA); and from centimetre-scale experiments in the Ice Physics laboratory at UCL. We show that the effective kinetic friction is consistent across these scales, and comparable to friction coefficients measured without rubble. Looking at static friction, we find that when floes are in static contact for a short time, the presence of rubble acts to reduce static friction. However, if floes and rubble remain in static contact for around 10^4s (a few hours) then the presence of rubble promotes strengthening, and the floe-floe effective friction can be raised by the presence of rubble. This has implications for modelling Arctic Ocean dynamics and for assessing friction loads on ships making repeated passages through a channel.

Introduction
To model the dynamics of sea ice, we need to consider how sea ice floes interact through fracture and friction across a range of scales (Sammonds and Rist, 2001). One part of this interaction is floe-floe in-plane sliding – i.e. large sheets of sea ice sliding past each other. To quantify resistance to this sliding, we need an understanding of friction. In some models of sea ice dynamics, ice friction has been set as a variable or tuning parameter (e.g. Hopkins and Thorndike, 2006). This is, in part, because the friction of ice on ice is difficult to model. A complete model would account for the microphysics of melting, brine drainage, adhesion, lubrication and fracture, for example (Hatton et al., 2009). Even then, the results could vary with ice type (first-year or multi-year, for example) and with temperature. Recent work modelling ice friction, therefore, has looked for patterns in the sliding behaviour of ice, rather than focussing on a single friction coefficient.

Schulson (2018) shows data from twelve recent studies which support a model of velocity strengthening (i.e. friction increases with increasing sliding speed) at speeds below around 10^{-5}-10^{-4}ms^{-1}, and velocity weakening (friction decreases with increasing sliding speed) above this threshold. Schulson (2018) also separates experiments by roughness (specifically, by how the ice surfaces were prepared) and notes that friction appears to have a greater sensitivity to changes in roughness in the velocity weakening regime. Schulson (2018) goes on to suggest that the cause of the increased sensitivity at higher sliding speeds is due to sliding-induced fragmentation, where rougher surfaces produce larger fragments. The effect of this roughness or fragmentation is pronounced: at sliding speeds of 10^{-2}ms^{-1}, rougher ice has a friction coefficient around 0.6, while smoother ice has a friction coefficient around 0.06. This work is in contrast to Hatton et al., 2009, who investigated the effect of ice surfaces on ice friction, and found experimentally that "surface topography is controlled by the sliding process, not by … the cutting method initially used to produce the faults." Perhaps, as suggested by Schulson (2018), the important difference is not the eventual ice surface, but the possibility of ice fragments being dislodged, and acting as an intermediate layer between the two surfaces.

Lishman et al. (2011) and Lishman et al. (2013) show results from experiments on ice-ice sliding with varying sliding speeds, alongside slide-hold-slide (SHS) tests and acceleration-deceleration tests. These results show that ice friction has memory: the instantaneous friction coefficient depends not just on the instantaneous conditions, but also on what has gone before. By analogy with earlier experiments on sliding in rocks (Ruina, 1983), we can say that friction depends on the *rate* of sliding and also on the *state* of the sliding interface.

In this work, we show results from slide-hold-slide tests, and tests with varying sliding speeds, conducted on ice-rubble-ice interfaces. These can then be compared directly with literature results from experiments which were conducted on ice-ice interfaces. In this way we can begin to test the hypothesis that ice fragmentation, and the presence of ice rubble, has a significant effect on sea ice friction.

One useful point of comparison is the literature on the effect of gouge on sliding in rock faults. A number of studies have compared rock-rock sliding and rock-gouge-rock sliding. Gouge material is the product of wear along sliding surfaces, and is naturally produced along faults when sliding occurs (Marone et al., 1990). Research has mainly focused on the presence and effects of gouge in rock systems, with the aim of understanding the dynamics of rock faults on tectonic scales. Studies on rock have shown that gouge generation at initially bare faults results in an increase in frictional resistance (Byerlee, 1967; Scholz et al., 1972). There is evidence to suggest that the presence of gouge stabilises sliding (Byerlee and Summers, 1976; Scholz et al., 1972; Marone and Scholz, 1988) through shear localisation features which develop with increasing slip. Engelder et al. (1975) note that the transition from stick slip to stable sliding is accompanied by a transition from sliding occurring at the rock-gouge contact to sliding being accommodated by owing gouge. Increasing gouge thickness has the effect of increasing the normal pressure at which this transition occurs (Byerlee and Summers, 1976).

Marone et al. (1990) conducted experiments using quartz sand at a range of velocities with and without an initial gouge layer. Velocity strengthening behaviour was observed when an initial gouge layer was present, but velocity weakening behaviour was observed when it was not. They also report that the magnitude of strengthening in the former case varies directly with gouge thickness and surface roughness, and inversely with normal stress.

Mair et al. (2002) compared the effect of varying angularity and particle size distribution (PSD) of gouge (using sand and glass spheres) on kinetic friction and sliding behaviour. They found that a narrow PSD of spherical gouge material resulted in unstable, stick-slip sliding, whereas angular and wide-PSD spherical gouge produced stable sliding. Fracture of spherical grains was suggested as the reason why sliding with this gouge type becomes stable with accumulated slip. Mair et al. (2002) also observed lower friction coefficients for spherical particles compared to angular ones ($\mu \approx 0.45$ compared to 0.6), and attributed this to a low friction translation mechanism such as grain rolling.

Dieterich (1972, 1981) noticed that the coefficient of static friction became highly time-dependent when gouge was present between the sliding faces, and an approximate logarithmic increase in gouge strength with hold time was observed in his experiments on rock. Subsequent studies have provided further evidence for the time- dependence of static friction between rock surfaces separated by gouge material (Scholz et al., 1972; Marone, 1998).

Overall, then, we might expect that the presence of ice rubble might affect overall frictional resistance; the transition between velocity-strengthening and velocity-weakening regimes; the development of

stick-slip cycles in sliding; and the time-dependence of static friction. Further, we might expect that the shape and size of the rubble (which may in turn change during sliding) will be important inputs. We are not aware of systematic studies investigating how ice rubble affects ice sliding. Fortt and Schulson (2007) do note that a gouge-like material is expelled from the sliding interface in their experiments on freshwater ice.

In this paper we present results from ice-rubble-ice sliding experiments in the laboratory, in the ice basin, and in the field. This range of experimental configurations allows us to make comparisons across scales.

Centimetre-Scale Laboratory Experiments

Double-direct shear experiments on the centimetre-scale were performed in the Ice Physics Laboratory at UCL using laboratory-grown saline columnar ice. The laboratory setting allowed for greater control of the set-up (for example, enabling the use of accurately measured ice blocks and rubble of a standardised size), and also for a greater control of the ambient temperature. Saline ice (water salinity 31ppt; bulk ice salinity 7-9ppt) was grown using an insulated cylinder, heated from below and cooled from above. The method is described, and example thin sections are shown, in Bailey et al., 2012.

Sliding experiments were conducted in a double-direct shear setup, as shown in figure 1. Three ice blocks, separated by two regions of ice rubble 12 mm wide, were arranged in the vertical plane inside a load frame which applied a normal force. The central, moving ice block is 150mm (high) x 50mm (wide) x 80mm (deep), and the fixed ice blocks are 80mm x 90mm x 80mm. Ice rubble was prepared by sieving broken lab-grown ice using two graduated sieves, so that the diameter of ice rubble grains were in the range 5.6-6.7mm. This rubble size was chosen because it allowed three to four layers of rubble to fit in the gaps between middle and outer ice blocks, which is comparable to other experiments in this paper.

A shear force, applied by an actuator piston and detected by an in-line load cell (model 614 tension-compression Tedea Huntleigh, accuracy ±0:1%), was applied to the middle block in order to push it through the two outer ice blocks, and its displacement was measured by a linear actuator (model PZ-34-A-150 Gefran, accuracy ±0:075 mm). The force was evenly distributed across the middle block's top surface by a load spreading plate which was situated between the middle block and the load cell. A normal force was applied across the set-up via two side load panels, which controlled the load using a constant pressure hydraulic system. Perspex shims were placed underneath the outer ice blocks, and frozen onto their front and back (in the vertical plane) in order to confine the rubble to the rubble region. The load frame containing this set-up was contained in an environmental chamber in which the ambient air temperature was cooled using liquid nitrogen. This set-up was designed to be comparable to that used by Mair and Marone (1999) to investigate rock friction with a gouge.

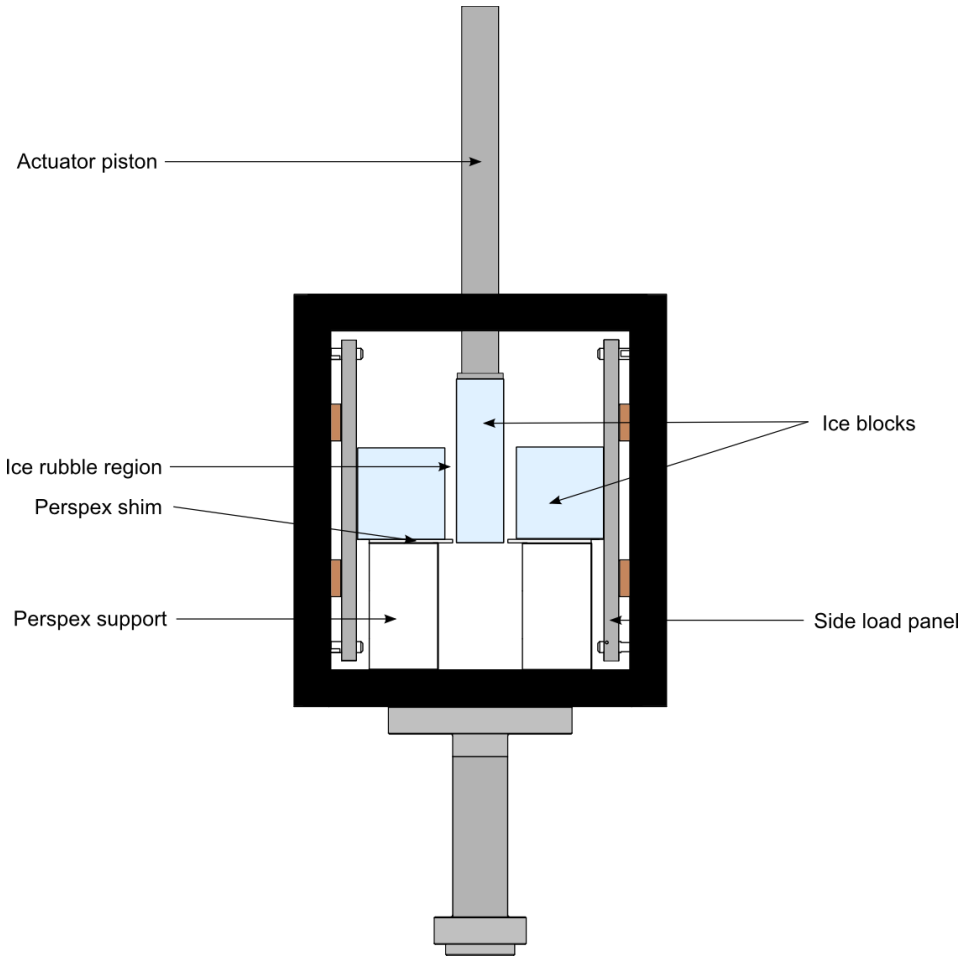

Figure 1: The load frame in which the ice blocks and rubble were arranged. Plates on either side of this load frame applied a normal force, and the entire load frame was placed in an environmental chamber which allowed the ambient air temperature to be controlled. The central, moving ice block is 150mm (high) x 50mm (wide) x 80mm (deep), and the fixed ice blocks are 80mm x 90mm x 80mm.

Figure 2 shows a set of results from a slide-hold-slide test, conducted at -7°C, using this setup. In this experiment, the middle ice block is moved at $10^{-4}ms^{-1}$ over distances of 6mm, punctuated by static periods lasting 1, 10 and 100s. Note that during hold periods, the actuator is moved away from contact with the ice, so that the middle block isn't moved when the actuator moves fractionally under hydraulic control. This "backing off" of the actuator accounts for the dips in pusher displacement seen around 150, 200 and 375s in the bottom graph of figure 2.

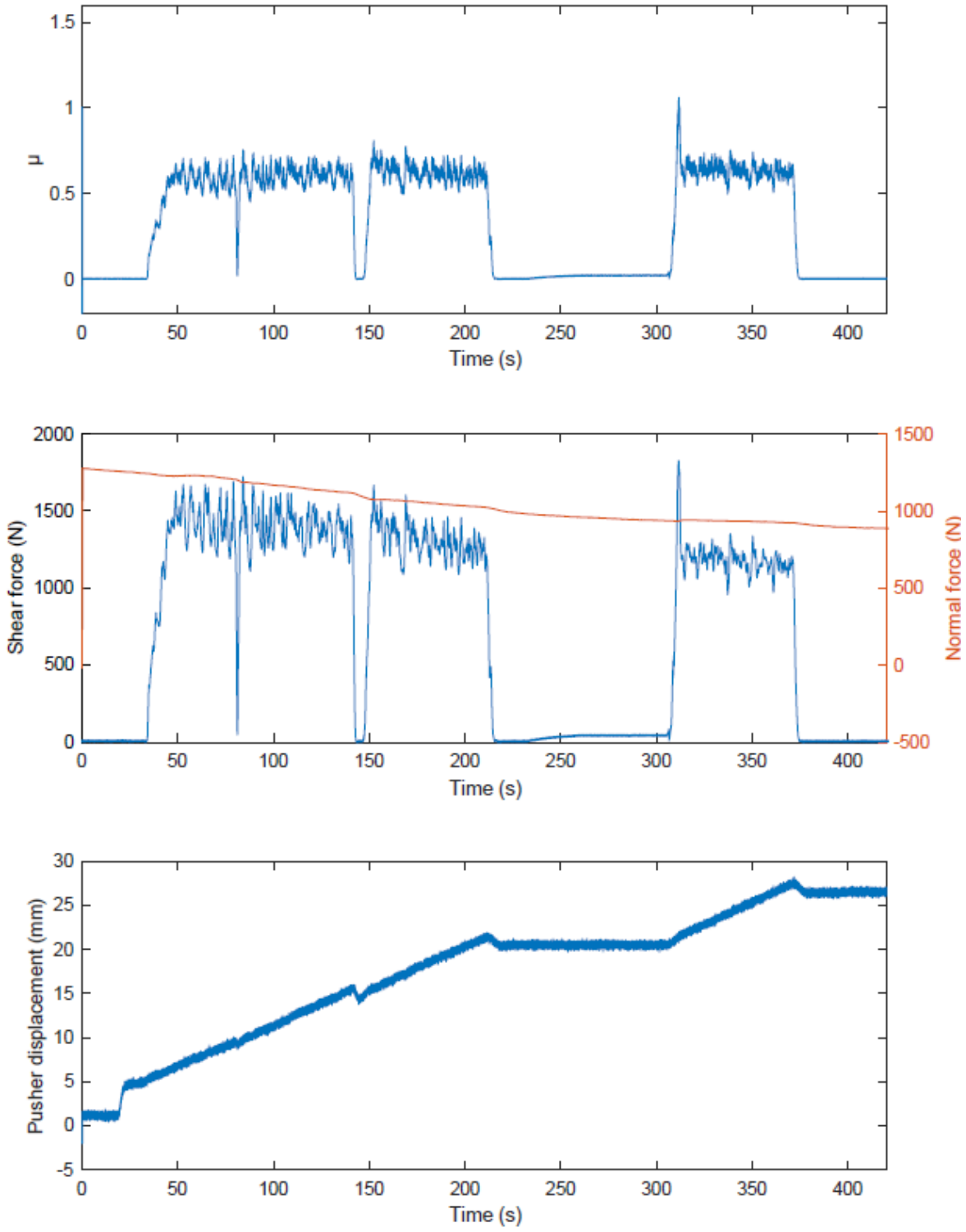

Figure 2: results from a slide-hold-slide experiment conducted at -7°C in the laboratory apparatus shown in figure 1. The top figure shows calculated friction as a function of time; the middle figure shows the measured shear force and normal force; and the bottom figure shows the measured pusher displacement (programmed pusher displacement is similar but less noisy). Static holds of 1s (at around 80s), 10s (at around 140s) and 100s (from 220-320s) are shown. Increases in friction can be seen on resumption of motion after the 10s and 100s static holds.

These results show stick-slip sliding around a fairly constant average friction coefficient, with higher friction coefficients immediately after static holds. Note that we experienced some drop off of normal force due to leaks in the hydraulic system. Friction coefficient μ is calculated as (shear force / (2 × normal force)), with the factor of two to account for the two separate sliding interfaces.

Laboratory results

Two summary graphs of the experimental results from the laboratory experiments are shown in figure 3 and figure 4. In figure 3, the effect of hold time in slide-hold-slide experiments is shown. The peak friction coefficient required to reinitiate motion increases with the length of the hold period. The effect of temperature here doesn't lead to consistent trends across hold times. At longer hold times, lower temperatures lead to greater strengthening. The second graph shows the relationship between friction coefficient and sliding velocity, and shows evidence of both velocity-strengthening and velocity-weakening, with a transition somewhere around $10^{-3}ms^{-1}$. Stick-slip behaviour is observed at 10^{-4}-$10^{-3}ms^{-1}$ (shown by the vertical bars on the graph) and is less pronounced at $10^{-2}ms^{-1}$.

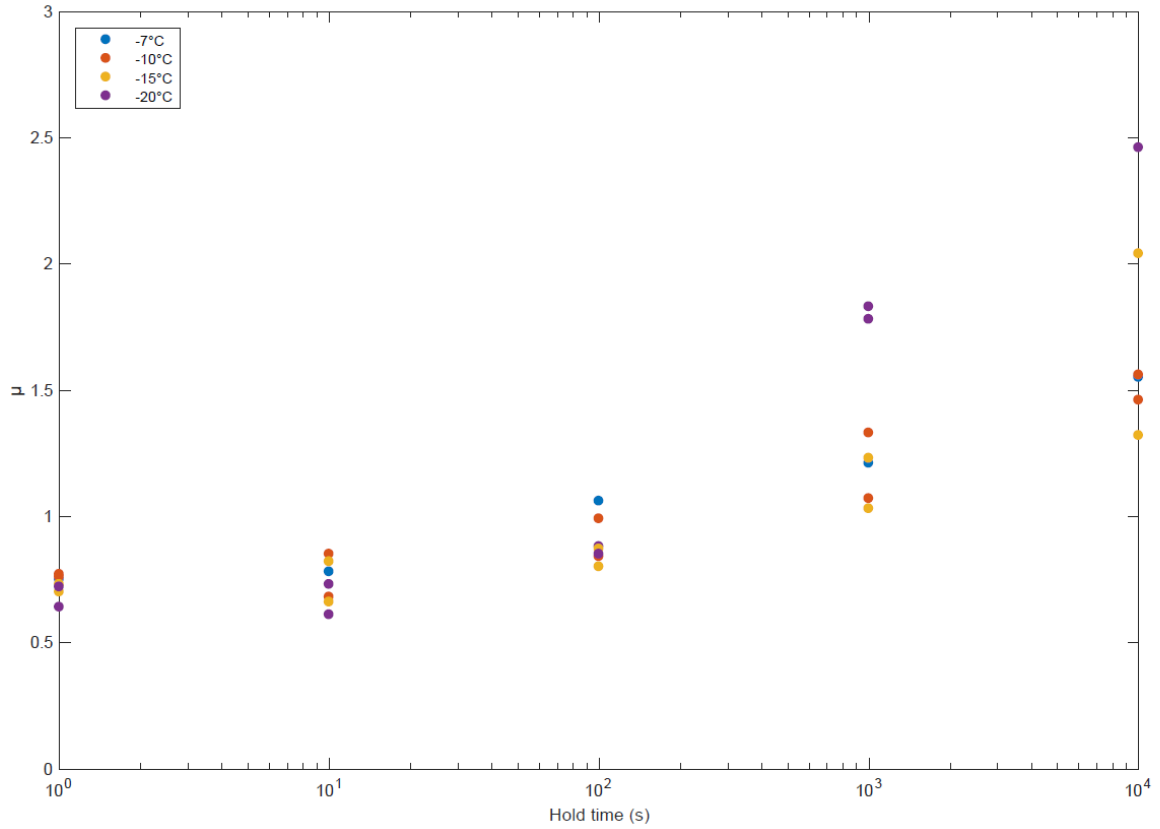

Figure 3: The effect of static hold time on peak friction in laboratory experiments across a range of temperatures. Some experiments were repeated, and multiple data points are shown for these experiments: this gives a sense of experimental variation in our results.

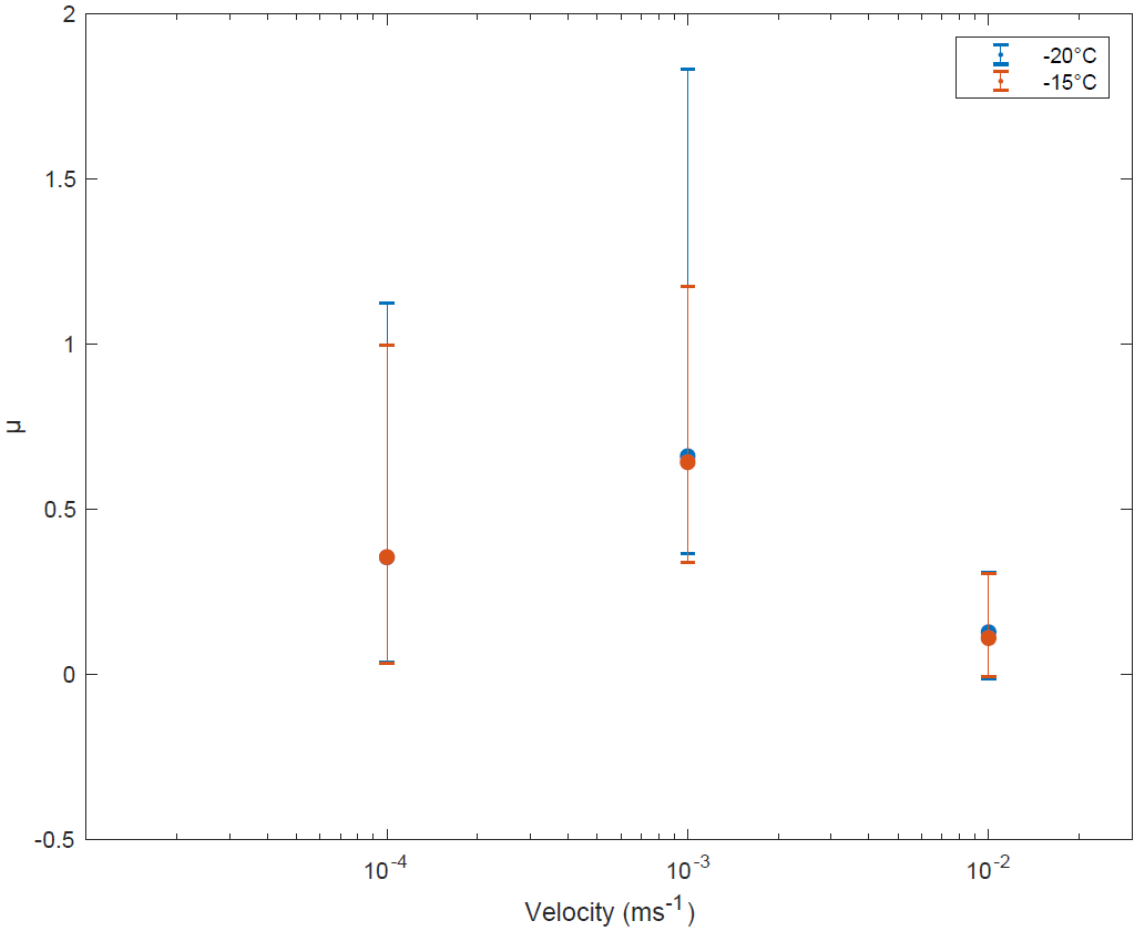

Figure 4: The relationship between μ and sliding velocity for temperatures of -15 and -20°C. Data points represent the mean kinetic friction during the period of steady sliding, and the maximum and minimum extent of vertical bars correspond to the highest and lowest kinetic friction experienced during this period. Higher vertical bars are associated with higher-amplitude stick-slip cycles.

Ice Basin Experiments

Double-direct shear experiments on the metre-scale were performed in the Large Ice Basin at HSVA using saline columnar ice grown *in situ*, following an approach described by Sammonds et al. (2019). The ice was formed from water of 6.8ppt salinity. Ice salinity was measured as 2ppt. The bulk density of the level ice was 920kgm^{-3}. The ice was formed over the course of one week at an air temperature of -18°C. All experiments were performed at an air temperature of -8°C. During the experimental programme, ice thickness grew from around 20cm to around 30cm. Thin sections (Scourfield, 2019) show a granular upper layer (grain size <1mm), around 15mm thick, with columnar ice below (grain size ≈1cm). Further ice properties, including details of ice strength can be found in Scourfield (2019).

The experimental set-up consisted of a mobile central ice block (3.5 m long, 1.5 m wide) in a channel of open water. Either side of this were ice rubble regions (1.5 m long, 0.5 m wide), bound on one side by the middle block, and on the other by floating ice beams. These beams ensured that the rubble regions were bound by ice on both sides at all times during sliding.

Wooden side load frames housing pneumatic rams were situated on both sides of the set-up next to the floating ice beams, and applied a normal force across the ice rubble regions and middle block. The degree of extension or retraction of the side load frames was measured by laser distance sensors (Di-

soric, type LHT 9-45 M 10 P3IU-B4, accuracy ±15 mm), situated at either end of both frames; from these measurements, information about the contraction or dilation of the rubble regions could be extracted. A pusher plate attached to the facility's moveable main carriage provided a shear force to the middle block to push it through the channel and past the ice rubble regions, in double-direct shear fashion. Using the shear force applied by the pusher plate, and the normal force applied by the side load frames, the coefficient of friction, μ, may be calculated as the ratio of shear force to normal force as before.

To maintain a two-dimensional problem (to simplify modelling), the rubble region consisted of just one layer of floating rubble pieces. The effects of ice rubble angularity were explored by repeating steady sliding and SHS experiments with four different rubble types - small round rubble (i.e. discs, 9.5cm diameter), large round rubble (16.5cm diameter), small diamond-shaped rubble (10cm short axis, 17cm long axis) and large diamond-shaped rubble (18cm short axis, 30cm long axis). All rubble pieces were 7-10cm thick (note that this means they are thinner than the surrounding level ice).

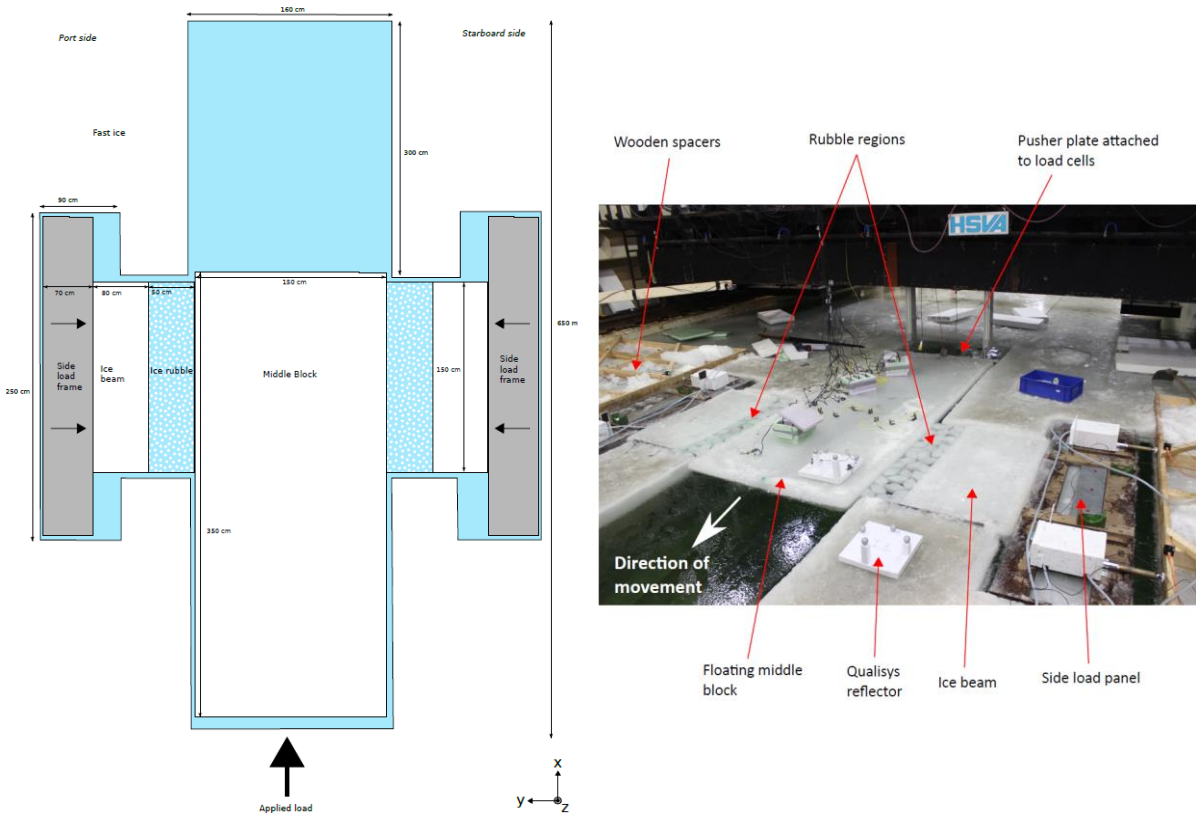

(a) (b)

Figure 5: experimental setup in HSVA.

Ice Basin Results

Summary results from ice basin tests are shown in the same format as those from laboratory tests. Figure 6 shows a set of results from an individual experiment, in this case sliding at 3mms^{-1}. Figure 7 shows peak static friction as a function of hold time across all experiments. Again, peak friction increases with hold time. In these experiments, though, we see a marked transition in peak friction between 10^3s and 10^4s hold times. Figure 8 shows average friction against sliding velocity for the ice basin experiments. Within the range of sliding speeds we tested (3×10^{-3}ms^{-1} – 10^{-1}ms^{-1}), we see velocity-weakening behaviour, i.e. the average friction decreases with increasing sliding speed.

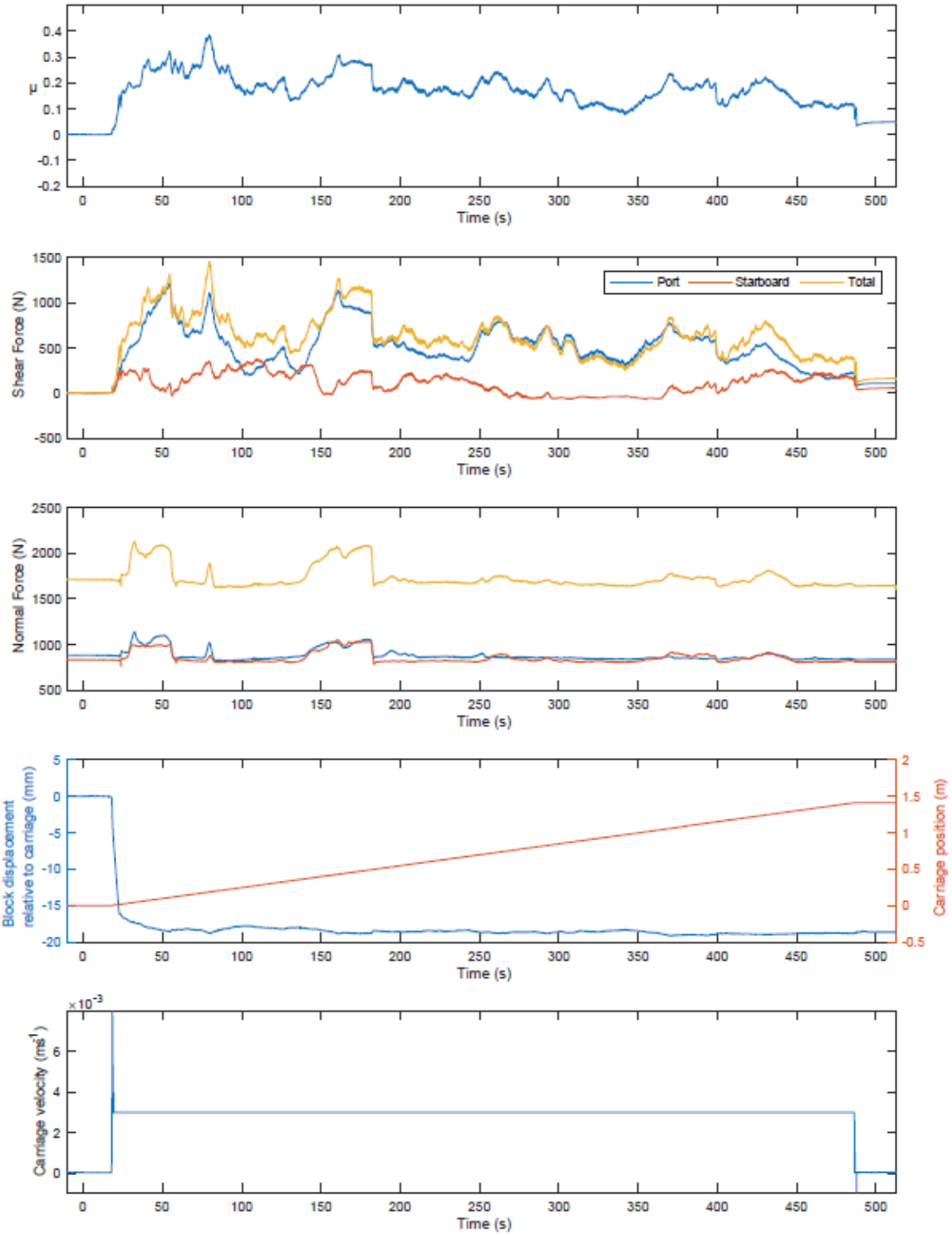

Figure 6: results from a steady-sliding experiment at HSVA. The top plot shows effective friction; the second plot shows measured shear forces; the third plot shows measured normal forces; the fourth plot shows the carriage position, and the relative displacement of the main sliding block relative to the carriage; and the final plot shows the carriage speed.

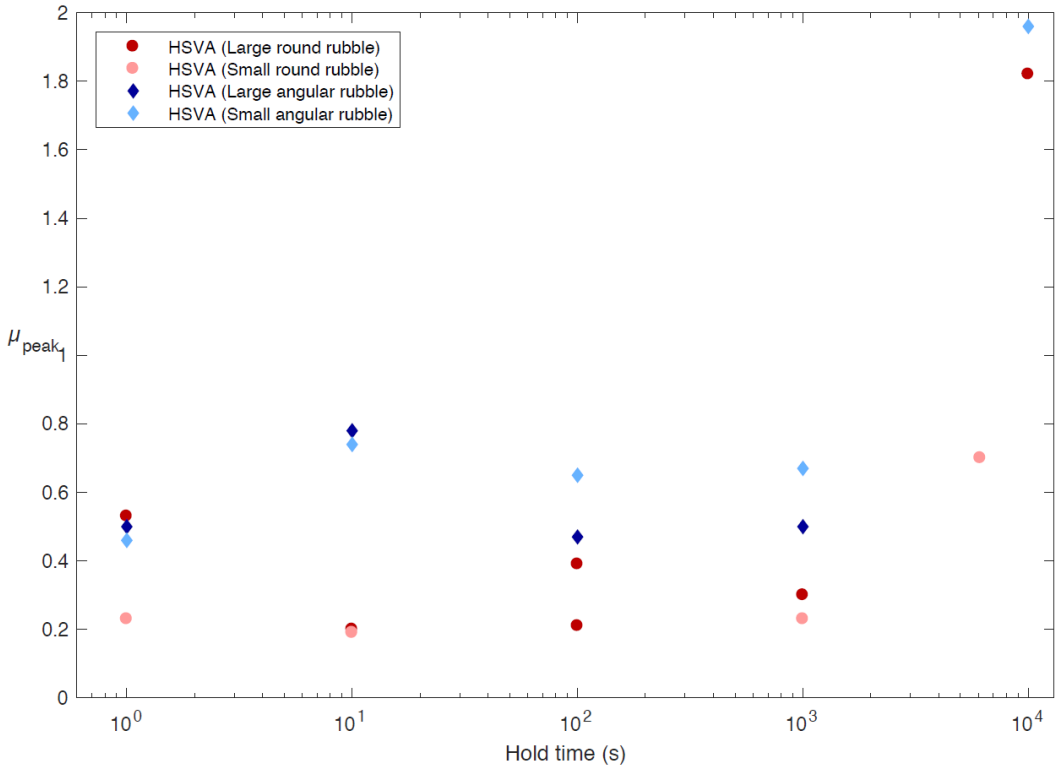

Figure 7: the relationship between hold time and peak friction in ice basin experiments.

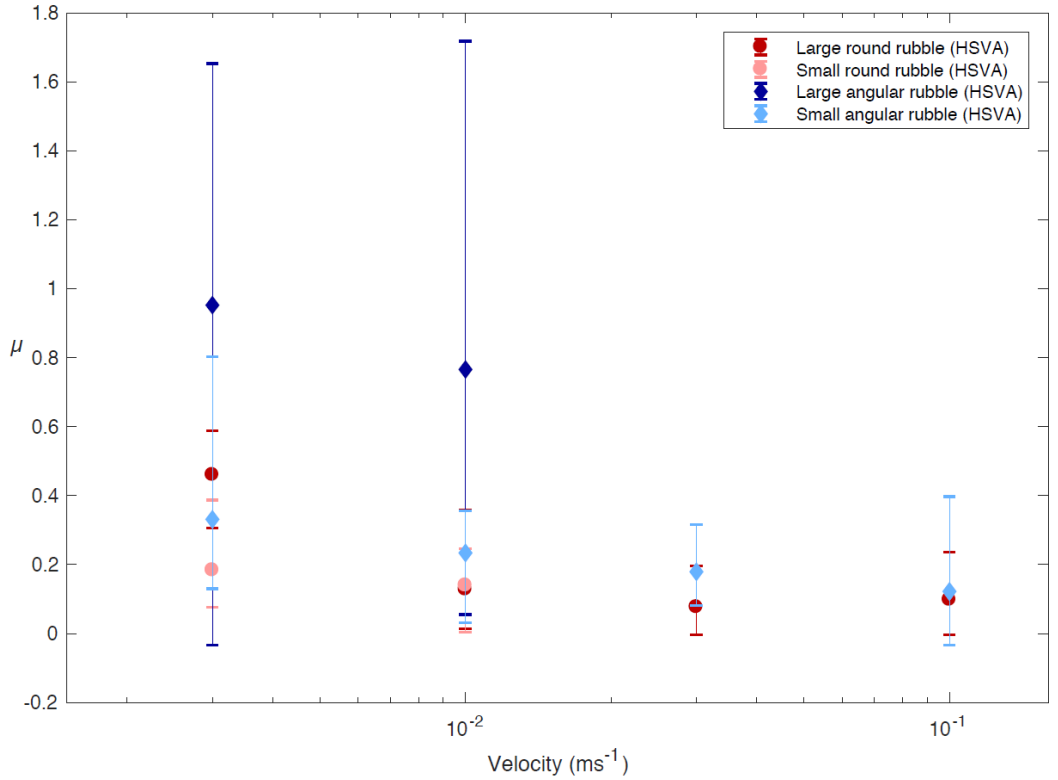

Figure 8: the relationship between sliding velocity and friction in ice basin experiments. Data points represent the mean kinetic friction during the period of steady sliding, and the maximum and minimum extent of vertical bars correspond to the highest and lowest kinetic friction experienced during this period. Higher vertical bars are associated with higher-amplitude stick-slip cycles.

Field Experiments

Double direct shear experiments were conducted in the Van Mijenfjorden, near the mining town of Svea, Svalbard in March 2015, following an approach described by Scourfield et al., 2015. Air temperatures during the experiments were between -11°C and -17°C. The ice used in the experiments is natural sea ice, formed from water with measured salinity of 30ppt. The thickness of the level ice was around 60cm. The experiments are conducted in a double shear configuration similar to that used in the lab and ice basin experiments. Ice rubble in these experiments is used by breaking up ice blocks using axes. The aim in this procedure was to produce a roughly fractal ice volume distribution. The largest pieces of ice were approximately 200mm on each side. The ice rubble regions are approximately 300mm deep. Side load was applied by a floating hydraulic load frame, and normal load was supplied by a mains-powered electrical actuator: the actuator speed for slide-hold-slide experiments was ~$6x10^{-3}ms^{-1}$. All the ice edges were saw-cut by hand. The experimental setup is shown in figure 9, and a typical set of results for a slide-hold-slide experiment is shown in figure 10.

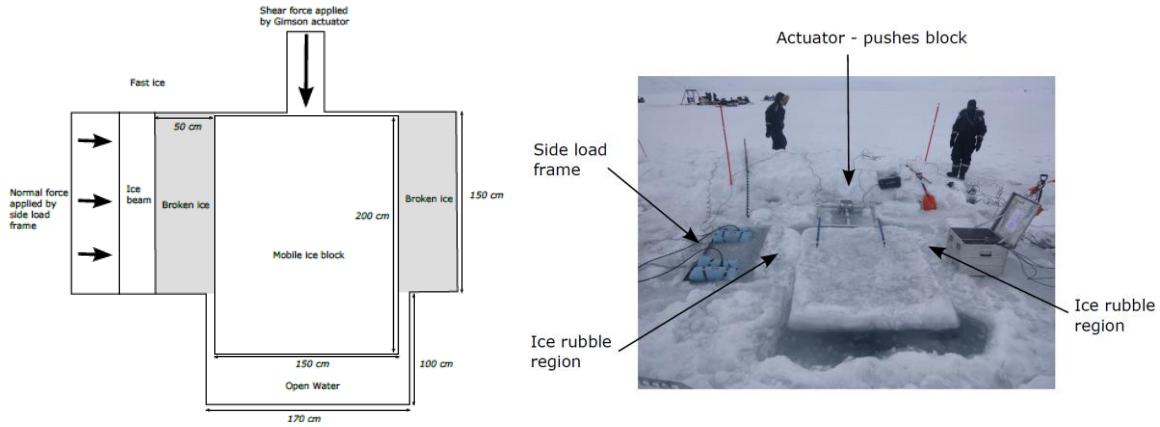

(a) (b)

Figure 9: the experimental setup for field experiments.

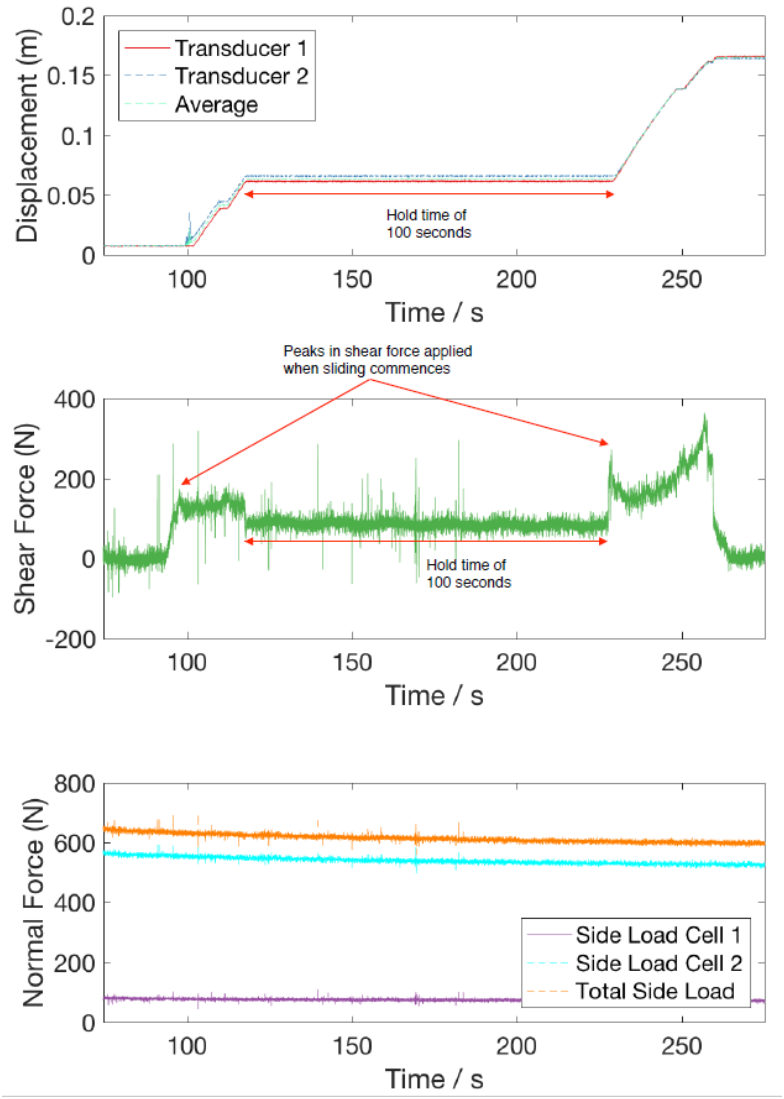

Figure 10: Representative data for a SHS steady sliding test conducted in Svea, showing a period of sliding, followed by a 100s hold time, followed by a second period of sliding.

Field Results

Data from field experiments is shown in figures 11 and 12. These results are shown in the same format as results for lab and ice basin experiments: the first graph shows peak friction as a function of hold time, and the second graph shows average friction as a function of sliding velocity. We see peak friction increases with hold time, with a marked increase in peak friction between 10^3 and 10^4s. One further experiment, with a hold time of 6.5×10^4s, overnight, led to a shear force around 200 times greater than the normal force. This data point is not plotted as it distorts the axes, and also because it might be considered outside the scope of friction models (since the ice was fully consolidated.) Nevertheless, we note it here as evidence that the peak friction coefficient keeps on rising at longer hold times than those shown in figure 11.

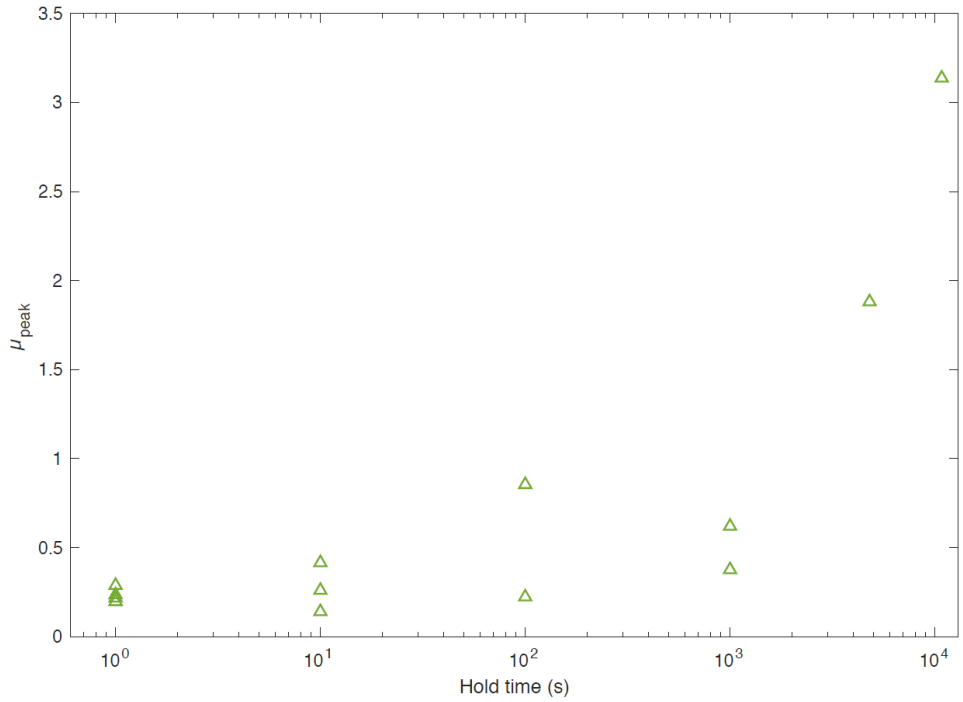

Figure 11: the relationship between peak friction and hold time. Not shown here (since it leads to a distorted y-scale) is a data point from an 18-hour (6.5×10^4s) hold time, where the shear force was found to be a factor of nearly 200 greater than the normal force (i.e. $\mu_{peak}\approx200$; see later discussion of whether this should be modelled as friction.)

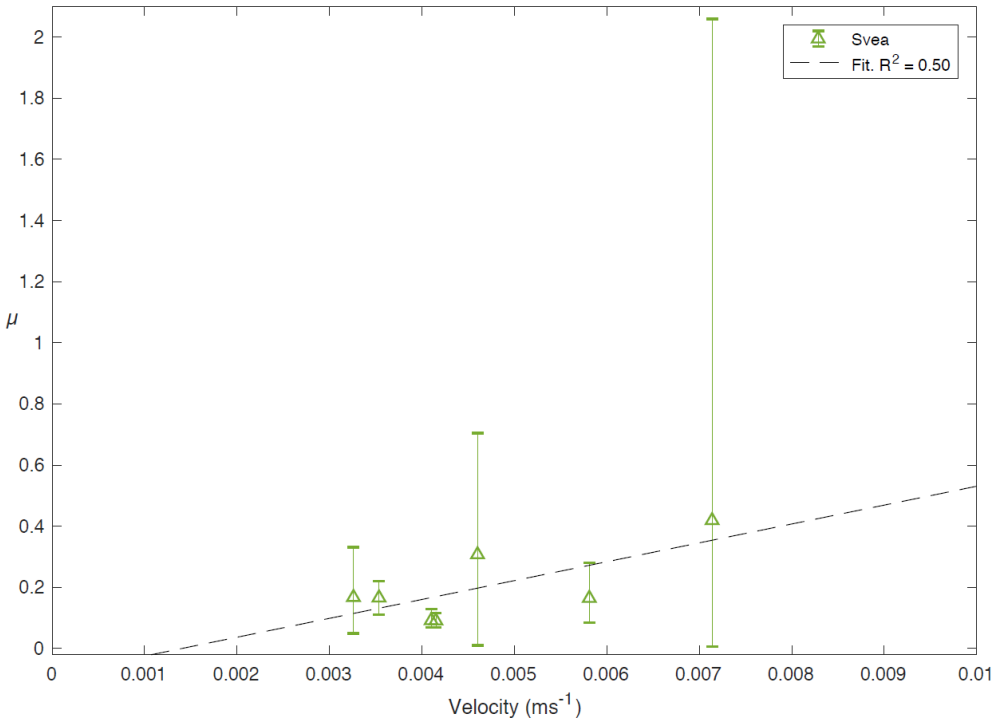

Figure 12: the relationship between friction and sliding velocity. Data points represent the mean kinetic friction during the period of steady sliding, and the maximum and minimum extent of vertical bars correspond to the highest and lowest kinetic friction experienced during this period. Higher vertical bars are associated with higher-amplitude stick-slip cycles.

Discussion

Experimental data have been presented across three scales, and three sets of experimental conditions. These sets of experiments are similar in configuration (double shear), and the slide-hold-slide experiments cover similar ranges of hold times (10^0 to 10^4s). Sliding speeds vary from experiment to experiment, according to the capabilities of the actuators. Temperatures vary somewhat between experiments, within the range -20 to -7°C. In each case we wished to produce results at around -10°C, to allow comparisons to be made at constant temperature; in the ice basin, the temperatures were kept slightly warmer to limit ice growth, and in the field, it was not possible to control temperature. Salinity is similar in the lab and field experiments (8-9ppt ice salinity), and lower in the ice basin experiments (ice salinity around 3ppt), because of limitations in the amount of salt which could be added to the ice basin. Differences in the orientation of experiments (i.e. on the horizontal plane in the field and ice basin, but on the vertical plane in the laboratory) and the presence of water (i.e. field and ice basin experiments performed using ice floating on water, but dry in the laboratory) should also be noted. Acknowledging these sources of variation between experiments, we still feel there is merit in comparing results from all experiments.

Time-dependent friction

As in the individual experimental results shown above, we first show the effects of varying hold times in slide-hold-slide experiments. In figure 13, alongside hold time results, we plot a theoretical model proposed by Schulson and Fortt (2013). This models explains static strengthening in terms of creep of asperities in contact.

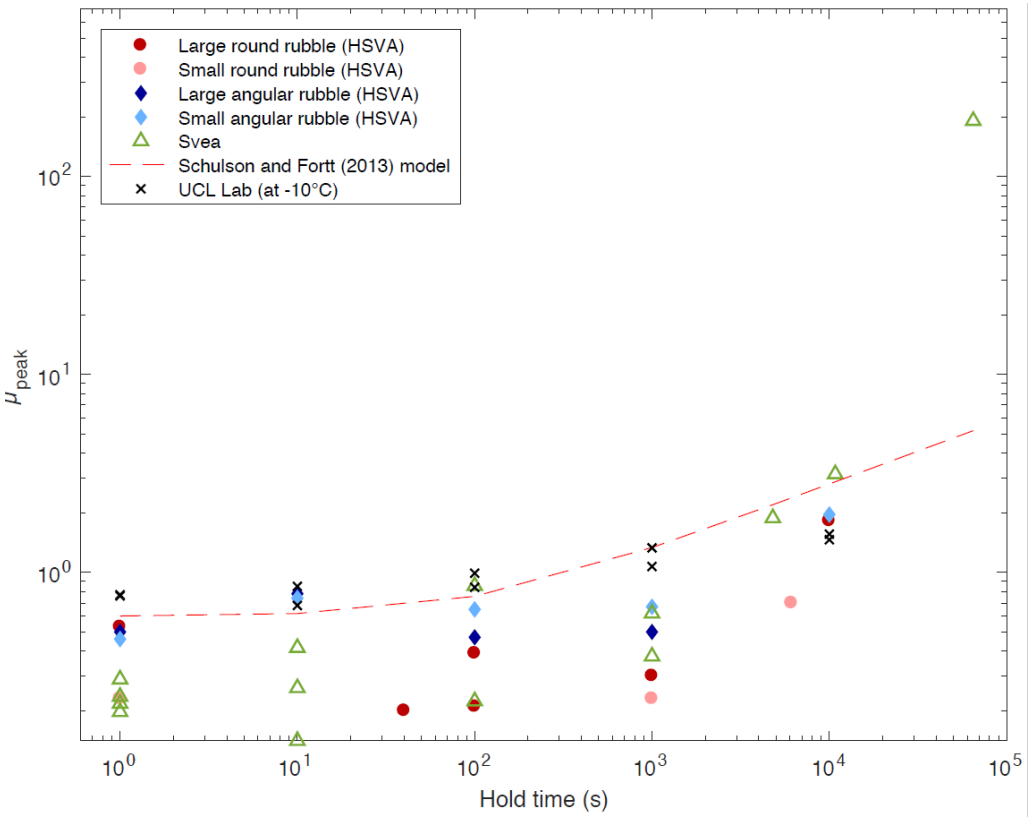

Figure 13: relationship between hold time and peak friction, compared across all experiments, and to ice-ice model proposed by Schulson and Fortt.

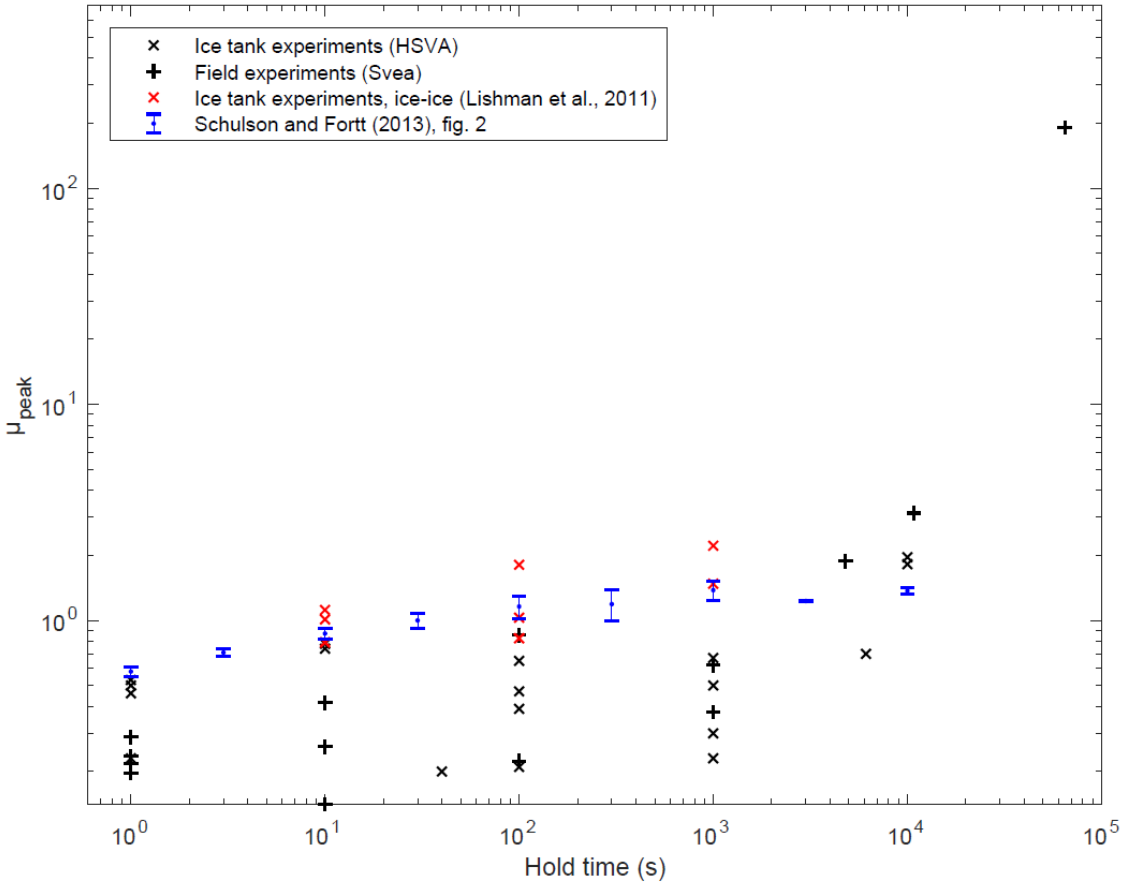

Figure 14: relationship between hold time and peak friction, comparing ice-ice sliding to ice-rubble-ice sliding. Black markers show results from this study. Red markers show results from Lishman et al. (2011). Blue markers show results from Schulson and Fortt (2013).

In figure 14, we show the results from this ice-rubble-ice study (black data points) compared to results from previous studies of ice-ice sliding (Lishman et al. (2011), red data points; Schulson and Fortt (2013), blue data points).

Two outcomes can be seen in comparing the slide-hold-slide results from this paper to previous ice-ice results, and to the ice-ice model of Schulson and Fortt (2013). First, at low hold times ($<\approx 10^3$s), the presence of ice rubble appears to reduce the static friction coefficient. The ice-ice experiments shown by red 'x' markers, and the ice-rubble-ice results shown by black 'x' markers show evidence that rubble decreases friction at hold times up to 10^3s. Second, at higher hold times ($>\approx 10^4$s), the presence of ice rubble appears to increase the static friction coefficient: the black markers in figure 14 curve upwards (on a logarithmic scale) at hold times greater than 10^3s, in a way which isn't seen in the ice-ice data in Lishman et al., 2011 or Schulson and Fortt, 2013. The behaviour is, however, a reasonable match for the ice-ice model (dashed red line in figure 13). In fact, the ice-rubble-ice data seems to fit the shape of the model more closely than ice-ice data does (cf. Schulson and Fortt (2013), figure 2).

The lab data in this study also shows a slight upwards curve (see figure 3), although this curve is less pronounced than for the field and ice tank data. The lab data also have higher friction values at low hold times, probably because the sliding between the hold times occurs at lower speeds. For this reason, the laboratory data are not shown in figure 14.

In summary, data from previous studies fall in straight lines on figure 14, while data from the laboratory (figure 3), ice tank (figure 7) and field (figure 11) in this study form upwards-trending curves.

The first outcome (that friction at low hold times may be lower for ice-rubble-ice sliding than for ice-ice sliding) makes some intuitive sense. The presence of ice rubble increases the number of pathways across which ice can slide. If one interface starts to stick, for any reason, then sliding can transfer to other interfaces. In some cases, sliding can also be replaced by rolling, which will also reduce static friction. Overall, cohesion is determined not by the strongest points of consolidation, as in ice-ice sliding, but by the weakest points – hence strengthening occurs more slowly. The most direct evidence for this weakening effect of rubble is in the comparison of ice-ice tests at HSVA (red markers on figure 14) with ice-rubble-ice tests at HSVA (black markers on figure 14).

The second outcome (that friction at higher hold times may be higher for ice-rubble-ice sliding than for ice-ice sliding) seems less intuitive, and the evidence presented here is less robust. The results in this study – specifically, those from the ice basin and from the field – show a discontinuity in friction at hold times of around 10^4s (i.e a few hours). Peak friction increases above the trend shown at lower hold times. This effect is not observed in data from previous studies on ice-ice sliding: in particular, there is no trace of it in experimental data from Lishman et al. (2011) or Schulson and Fortt (2013). This result suggests that ice-rubble-ice interfaces develop mechanical strength more quickly than ice-ice interfaces, when examined on a timescale of hours.

The exact process of mechanical strengthening, in either direct ice-ice friction or in ice-rubble-ice friction, is still not fully understood. Increased friction after hold times is observed in experiments with no melt, and can be explained by creep of asperities (see e.g. Dieterich, 1979). However, in ice friction experiments the possibility also exists for freeze bonds to develop between sliding surfaces (Repetto-Llamazares et al., 2011), and for formation, through freezing, of a new ice matrix, linking previously separate ice blocks into one new solid block. In each of our hold time experiments, we believe that each of these three forms of strengthening – asperity creep, freeze bonds between surfaces, and freezing of interstitial water – occur, and affect the development of friction. The second two forms of strengthening might, in other contexts, be considered outside the realms described by friction models. In applications of ice friction, though, freeze bonding and freezing are likely to play important roles in practical situations, and so we consider it useful to try to incorporate them into ice friction models. This complexity of ice friction (that asperity-deformation type friction seems inseparable from effects of freezing and consolidation) means that forces involved in our experiments can grow over orders of magnitude, leading to plots like figures 13 and 14 where friction (or, at least, the ratio of normal force to shear force) is presented on a logarithmic axis.

Most data collected so far, in this study and others, cover hold times up to 10^4s. At some long hold times, we expect that ice will have mechanically consolidated, and behave as a solid ice sheet, without any interface (see Bailey et al. (2012) for discussion of mechanical consolidation between vertically stacked ice sheets, a different but related problem). At this stage, we would not expect the strength of the ice to vary with further increases in hold times. Once mechanical consolidation has occurred, friction models (models which measure ratios of shear force or stress to normal force or stress) are not likely to be appropriate ways of understanding the shear strength of the ice sheet.

This behaviour is summarised in figure 15.

- In region 1 covering low hold times, rubble acts to weaken the sliding interface, by providing multiple sliding pathways and allowing rolling of rubble to replace sliding. The evidence for this weakening is presented in figure 13.
- In region 2, covering intermediate hold times (around 10^4-10^5s), the ice-rubble-ice interface gains mechanical strength faster than the ice-ice interface. Tentative evidence for this transition is provided in this paper, in particular by the high-friction data points towards the right hand side of figures 7 and 11. Experimental evidence in this region is difficult to collect, since high friction leads to high forces, which can damage equipment. More data are required in this region.
- In region 3, at high hold times, we are not aware of any experimental data which are directly comparable to data for regions 1 and 2. We make two proposals about this region. First, we believe that as $t \rightarrow \infty$, the two lines should converge. Second, we propose that friction models are not appropriate ways of understanding or predicting the behaviour of the interface in this region.

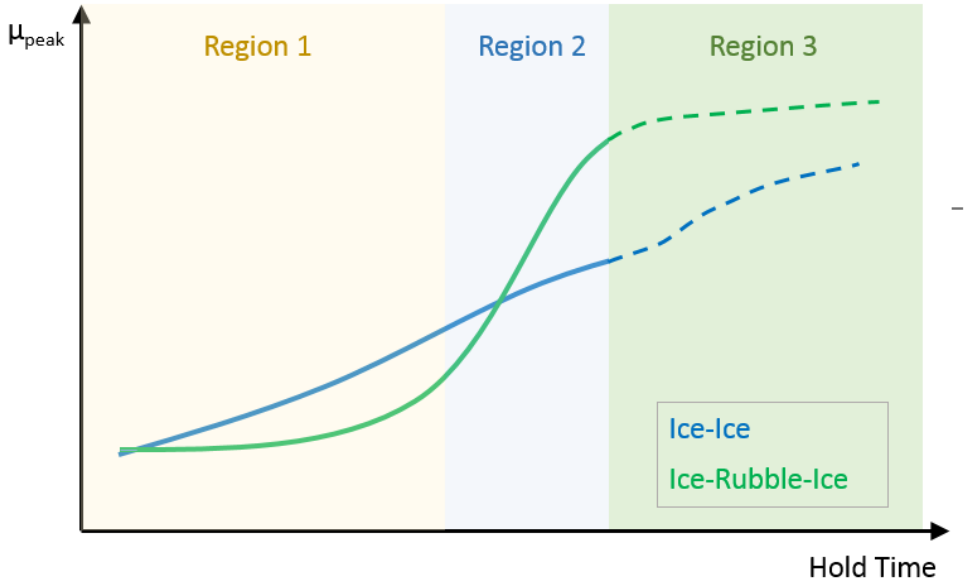

Figure 15: schematic diagram showing the effects of hold time on ice-ice interfaces (blue line) and on ice-rubble-ice interfaces (green line).

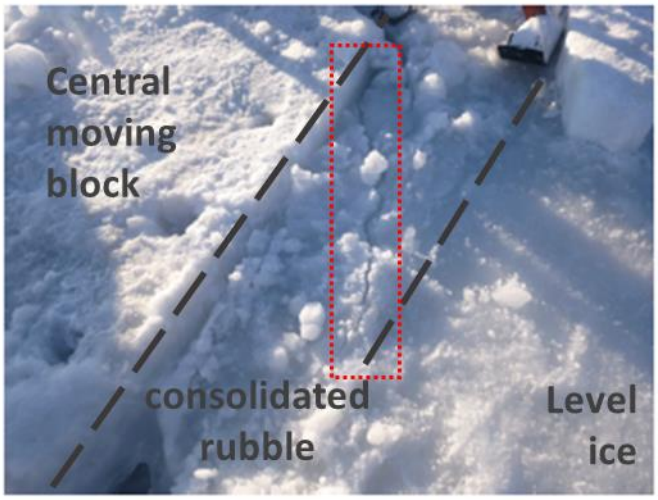

Figure 16: evidence of fracture (crack shown highlighted by red dotted box) within the consolidated rubble region as a result of the application of shear force after a hold time of 18 hours.

Figure 16 shows a photo of the effects of resuming sliding after an 18-hour hold during experiments in Svea. Motion does not occur by sliding on an interface parallel to the block and level ice edges, as in most sliding cases. Instead, a crack passes through the rubble region, at an angle of 30-45° to the direction of force, as might be expected in the failure of level ice. This data point gives some indication of where the transition between region 2 and region 3 occurs (after 18 hours, the ice rubble behaves somewhat like level ice, i.e. region 3), and also supports the idea that in region 3, the ice rubble behaves like a solid sheet rather than like a pre-existing sliding interface.

Velocity-dependent friction

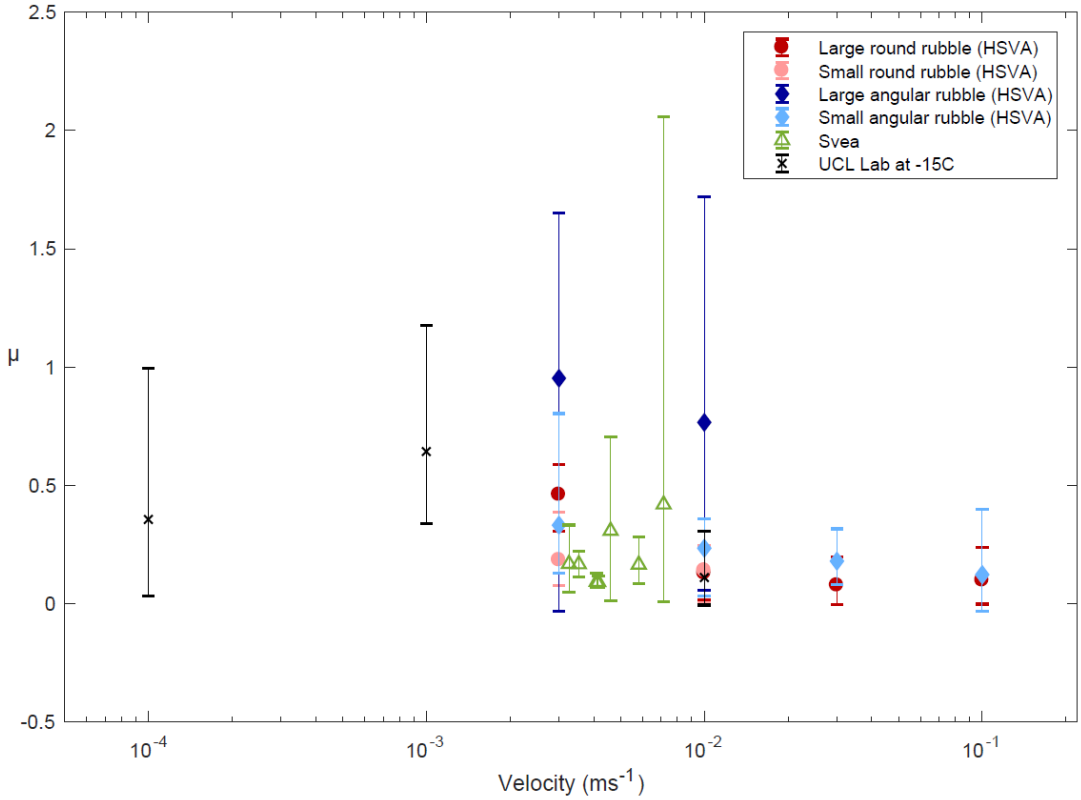

Figure 17: relationship between sliding velocity and friction, compared across all experiments. Data points represent the mean kinetic friction during the period of steady sliding, and the maximum and minimum extent of error bars correspond to the highest and lowest kinetic friction experienced during this period.

Figure 17 shows all results from this paper for friction as a function of sliding velocity. These results are broadly consistent with each other, and also with the results presented in Schulson (2018). With ice-rubble-ice sliding, the highest friction coefficients are seen at speeds between 10^{-3} and 10^{-2}ms^{-1}. Results for large angular rubble – blue diamonds – fall close to the rough-surface results presented by Schulson. Other results fall between Schulson's rough-surface grouping and the smooth-surface grouping. This provides some support for the hypothesis that fragmentation from rough-cut surface may be an important control on friction. Initial fragments from such surfaces are likely to be angular, and hence cause an increase in friction similar to the increased friction we see in this study. The data presented here do not show pronounced velocity-weakening above 10^{-4}ms^{-1}, which again suggests these ice-rubble-ice interfaces are more closely related to rough-cut ice interfaces than to the smooth surfaces.

We note that there is significant scatter within the velocity-dependent data we present, and that the different studies overlap but don't all follow the same trends. For example, the field data from Svea show velocity strengthening up to 10^{-2}ms^{-1}, whereas the ice tank data from HSVA show velocity weakening in this region. It's also worth noting that we can only present very limited data at low sliding speeds (due to limitations on the actuator and carriage controls in Svea and HSVA respectively).

Suggestions for further work

Several aspects of ice-rubble-ice friction are not discussed in this work. For simplicity, the rubble has been made using a similar process within each family of experiments, but further experiments might investigate the effects of rubble size, rubble size distribution, and porosity. Slush – tiny particles of

floating ice – seems to play an important part in promoting consolidation, and should be investigated. Data at low sliding speeds are limited in the present paper, and more data here would give a clearer picture of the transition between velocity-strengthening and velocity-weakening regions.

Implications for understanding sea ice dynamics

Over time, and with continued sliding, we expect ice to be abraded and wear away. This happened in all the experiments described in this paper. Examples from the ice basin and the field are shown in figure 18. In both cases, sharp corners are rounded down during experiments. This means that the rubble pieces tend to become more spherical. If angular rubble leads to higher friction than rounded rubble, and rubble tends to become less angular during frictional sliding, then we expect that average friction might decrease during prolonged frictional sliding of natural ice-rubble-ice interfaces.

(a)

(b)

Figure 18: ice before and after experiments in (a) the ice basin, and (b) the field. In both cases, freshly made ice rubble is shown on the left. The right-hand container in each image shows ice which has been through a sliding experiment.

Improved understanding of ice-rubble-ice interfaces, as described above, may help to increase our understanding of how natural sea ice slides. When sea ice floes break up, rubble forms. Further, the ice edges which form are likely to be rough, which means further fragmentation and rubble production is likely, as described above. The presence of rubble will mean that short term memory – static friction from short hold times – is likely to be reduced, compared to ice-ice interfaces. Mechanical consolidation of ice-rubble-ice interfaces may occur more quickly than for ice-ice interfaces. Over prolonged sliding, the ice rubble will abrade and become more spherical, and this will lead to reductions in the sliding friction. Direct observations of the evolution of ice-ice interfaces and ice-rubble-ice interfaces in nature (either on small scale through ship-based or land-based observation, or on large scale through aerial or satellite observation) will help to test the predictions in this paper and provide a further scale across which data can be compared.

Conclusions

We show results from experiments on the sliding of ice surfaces separated by ice rubble, across three different scales and environments. On the metre-scale, the presence of ice rubble lowers the coefficient of static friction (compared to ice-ice sliding) at hold times $<\approx 10^3$s. This is because the

rubble offers multiple pathways for movement, so that the static friction is dependent on the weakest cohesion, rather than the strongest. At higher hold times, experiments in the ice basin and the field suggest that rubble leads to a transition to rapid strengthening, so that ice-rubble-ice interfaces can be stronger than ice-ice interfaces for a given hold time. This would suggest that vertical planar ice-ice interfaces reach mechanical consolidation more slowly than aggregations of ice rubble. At very high hold times ($t>\approx10^5$s) friction becomes a less useful model for understanding the strength of the interface. During constant sliding experiments, ice-rubble-ice experiments show comparable results to ice-ice sliding experiments. Results with diamond-shaped rubble blocks are similar to results with sliding of rough-cut ice-ice interfaces, suggesting that fragmentation and rubble interference may play a part in the sliding of rough ice-ice interfaces. This has implications for the sliding of natural sea ice, which fractures into rough ice surfaces: in turn, these ice interfaces will fracture, leading to ice-rubble-ice sliding.

Acknowledgements
We would like to thank Aleksey Marchenko and the University Centre in Svalbard (UNIS) for the opportunity to join the Lance RV cruise, and for guidance and the substantial logistical support during fieldwork in Svea. We also acknowledge and thank the Research Council of Norway for funding field work through the SFI SAMCoT. We would like to thank Mark Shortt, Aleksey Marchenko, Ellie Bailey and Sammie Buzzard for assistance with the experiments at HSVA and Neil Hughes, Steve Boon and John Bowles for assistance with laboratory experiments at UCL. We would like to thank Kaj Riska (TOTAL SA) for advice and continual support.

The work described in this publication was supported by the European Community's Horizon2020 Research and Innovation Programme through the grant to HYDRALA-PLUS, Contract no. 654110. The authors would like to thank the Hamburg Ship Model Basin (HSVA), especially the ice basin crew, for the hospitality, technical and scientific support and the professional execution of the test programme in the Research Infrastructure ARCTECLAB.

SS was supported by a UCL Impact Studentship funded by the Institute for Risk and Disaster Reduction and TOTAL S.A.

References
Bailey, E., Sammonds, P. R., & Feltham, D. L. (2012). The consolidation and bond strength of rafted sea ice. Cold Regions Science and Technology, 83, 37-48.
Byerlee, J. D. (1967), Frictional characteristics of granite under high confining pressure, Journal of Geophysical Research, 72 (14), 3639-3648, doi: 10.1029/JZ072i014p03639.
Byerlee, J., & Summers, R. (1976). A note on the effect of fault gouge thickness on fault stability. In International Journal of Rock Mechanics and Mining Sciences & Geomechanics Abstracts (Vol. 13, No. 1, pp. 35-36). Pergamon.
Dieterich, J. H. (1972). Time-dependent friction in rocks. Journal of Geophysical Research, 77(20), 3690-3697.
Dieterich, J. H. (1979) "Modeling of rock friction: 1. Experimental results and constitutive equations." Journal of Geophysical Research: Solid Earth 84, no. B5 : 2161-2168.
Dieterich, J. H. (1981), Constitutive properties of faults with simulated gouge, Mechanical Behavior of Crustal Rocks, 24, 103{120, doi: 10.1029/GM024p0103.
Engelder, J. T., Logan, J. M., & Handin, J. (1975). The sliding characteristics of sandstone on quartz fault-gouge. pure and applied geophysics, 113(1), 69-86.
Fortt, A. L., & Schulson, E. M. (2007). The resistance to sliding along Coulombic shear faults in ice. *Acta materialia*, *55*(7), 2253-2264.
Hatton DC, Sammonds PR, Feltham DL. 2009 Ice internal friction: standard theoretical perspectives on friction codified, adapted for the unusual rheology of ice, and unified. Phil. Mag. 89, 2771–2799. (doi:10.1080/14786430903113769)
Hopkins, M. A., & Thorndike, A. S. (2006). Floe formation in Arctic sea ice. Journal of Geophysical Research: Oceans, 111(C11).
Lishman, B., Sammonds, P., & Feltham, D. (2011). A rate and state friction law for saline ice. Journal of Geophysical Research: Oceans, 116(C5).
Lishman, B., Sammonds, P. R., & Feltham, D. L. (2013). Critical slip and time dependence in sea ice friction. Cold Regions Science and Technology, 90, 9-13.
Mair, K., Frye, K. M., & Marone, C. (2002). Influence of grain characteristics on the friction of granular shear zones. Journal of Geophysical Research: Solid Earth, 107(B10), ECV-4.

Mair, K., & Marone, C. (1999). Friction of simulated fault gouge for a wide range of velocities and normal stresses. *Journal of Geophysical Research: Solid Earth*, *104*(B12), 28899-28914.
Marone, C., Raleigh, C. B., & Scholz, C. H. (1990). Frictional behavior and constitutive modeling of simulated fault gouge. Journal of Geophysical Research: Solid Earth, 95(B5), 7007-7025.
Marone, C., & Scholz, C. H. (1988). The depth of seismic faulting and the upper transition from stable to unstable slip regimes. Geophysical Research Letters, 15(6), 621-624.
Marone, C. (1998). The effect of loading rate on static friction and the rate of fault healing during the earthquake cycle. Nature, 391(6662), 69.
Repetto-Llamazares, AHV, K V. Høyland, and K-U Evers. "Experimental studies on shear failure of freeze-bonds in saline ice: Part I. Set-up, failure mode and freeze-bond strength." Cold Regions Science and Technology 65, no. 3 (2011): 286-297.
Ruina, A. (1983), Slip instability and state variable friction laws, Journal of Geophysical Research, 88, 10,359–10,370, doi:10.1029/JB088iB12p10359.
Sammonds PR, Rist MA. 2001 Sea ice fracture and friction. In Scaling laws in ice mechanics and ice dynamics (eds JP Dempsey, HH Shen), pp. 183–194. Amsterdam, The Netherlands: Kluwer.
Sammonds P, Scourfield S, Lishman B, Shortt M, Bailey E, Marchenko A 2019 Sea ice dynamics: The role of broken ice in multi-scale deformation. In Proc. HYDRALAB+ Joint User Meeting pp. 166-171, May 2019, Bucharest, Romania.
Scholz, C., Molnar, P., & Johnson, T. (1972). Detailed studies of frictional sliding of granite and implications for the earthquake mechanism. Journal of geophysical research, 77(32), 6392-6406.
Schulson, E. M. (2018). Friction of sea ice. Philosophical Transactions of the Royal Society A: Mathematical, Physical and Engineering Sciences, 376(2129), 20170336.
Schulson, E. M., & Fortt, A. L. (2013). Static strengthening of frictional surfaces of ice. Acta Materialia, 61(5), 1616-1623.
Scourfield S, Sammonds P, Lishman B, Marchenko A 2015. The effect of rubble on ice-sliding. In: Proc. 23rd Int. Conf. Port and Ocean Engineering under Arctic Conditions, Trondheim, Norway, June 14-18, 2015
Scourfield, S, 2019. The influence of ice rubble on sea ice friction. PhD Thesis, University College London.